Structures containing Atg9A and the ULK1 complex independently target depolarized mitochondria at initial stages of Parkin-mediated mitophagy

Eisuke Itakura, Chieko Kishi-Itakura, Ikuko Koyama-Honda and Noboru Mizushima*

Department of Physiology and Cell Biology, Tokyo Medical and Dental University, Tokyo 113-8519, Japan

*Author for correspondence (nmizu.phy2@tmd.ac.jp)

Accepted 7 November 2011
Journal of Cell Science 125, 1488–1499

doi: 10.1242/jcs.094110

Summary

Mitochondria can be degraded by autophagy in a process termed mitophagy. The Parkinson-disease-associated ubiquitin ligase Parkin can trigger mitophagy of depolarized mitochondria. However, it remains to be determined how the autophagy machinery is involved in this specific type of autophagy. It has been speculated that adaptor proteins such as p62 might mediate the interaction between the autophagosomal LC3 family of proteins and ubiquitylated proteins on mitochondria. Here, we describe our systematic analysis of the recruitment of Atg proteins in Parkin-dependent mitophagy. Structures containing upstream Atg proteins, including ULK1, Atg14, DFCP1, WIPI-1 and Atg16L1, can associate with depolarized mitochondria even in the absence of membrane-bound LC3. Atg9A structures are also recruited to these damaged mitochondria as well as to the autophagosome formation site during starvation-induced canonical autophagy. In the initial steps of Parkin-mediated mitophagy, the structures containing the ULK1 complex and Atg9A are independently recruited to depolarized mitochondria and both are required for further recruitment of downstream Atg proteins except LC3. Autophagosomal LC3 is important for efficient incorporation of damaged mitochondria into the autophagosome at a later stage. These findings suggest a process whereby the isolation membrane is generated de novo on damaged mitochondria as opposed to one where a preformed isolation membrane recognizes mitochondria.

Key words: Autophagy, Mitophagy, Parkin, ULK1, Atg9A, LC3

Introduction

Mitochondria mediate various physiological processes, such as energy production, metabolism, hormone production, calcium storage and promotion of cell death. However, mitochondrial dysfunction is also involved in the pathogenesis of human diseases such as myopathy, various neurodegenerative diseases and cancer. Thus, quality control of mitochondria is important in both physiological and pathological settings and can be achieved at both protein and entire organelle levels. Whereas control at the protein level involves the ubiquitin–proteasome system and mitochondrial proteolytic enzymes, organelle-level control is believed to be accomplished by mitophagy, a particular type of macroautophagy (referred to as autophagy herein) (Youle and Narendra, 2011).

In mitophagy, a single mitochondrion or a cluster of mitochondria are sequestered by the isolation membrane to form an autophagosome (mitophagosome). The autophagosome eventually fuses with a lysosome, which leads to complete degradation of autophagosomal contents. It was recently demonstrated that a Parkinson's-disease-associated ubiquitin ligase, Parkin, is recruited from the cytosol to damaged mitochondria and promotes mitophagy (Narendra et al., 2008). Subsequent studies also revealed that PTEN-induced putative kinase 1 (PINK1), another mitochondrial protein associated with Parkinson's disease, is essential for recruitment of Parkin to depolarized mitochondria (Gegg et al., 2010; Geisler et al., 2010; Kawajiri et al., 2010; Matsuda et al., 2010; Narendra et al., 2010a; Rakovic et al., 2010; Vives-Bauza et al., 2010; Ziviani et al., 2010).

Although it has been shown that Parkin can ubiquitylate a broad range of mitochondrial outer membrane proteins (Chan et al., 2011; Chen et al., 2010; Gegg et al., 2010; Geisler et al., 2010; Poole et al., 2010; Tanaka et al., 2010; Wang et al., 2011; Yoshii et al., 2011; Ziviani et al., 2010), it remains to be elucidated how Parkin enables damaged mitochondria to be recognized by the autophagosome. Degradation of outer membrane proteins by the proteasome might promote mitophagy (Chan et al., 2011; Tanaka et al., 2010), but it does not seem to be essential for recognition by autophagosomes (Yoshii et al., 2011).

Another proposed model is that p62 (also known as sequestosome 1), which has both the microtubule-associated protein light chain 3 (LC3)-recognition sequence (LRS) and ubiquitin-associated (UBA) domain, serves as an adaptor that links ubiquitylated mitochondrial protein and the autophagosomal LC3 family of proteins (Ding et al., 2010; Geisler et al., 2010; Lee et al., 2010). This model, however, is also controversial; recent reports have suggested that p62 is not essential for mitochondrial recognition by the autophagosome, but rather is important for perinuclear clustering of depolarized mitochondria (Narendra et al., 2010b; Okatsu et al., 2010). The results of these studies raise the possibility that binding of p62 and LC3 is not the first recognition mechanism.

Journal of Cell Science

Formation of the autophagosome is governed by organized functions of autophagy-related (Atg) proteins. In both yeast and mammals, the Atg1/ULK1 kinase complex (Atg1–Atg13–Atg17–Atg29–Atg31 in yeast, and ULK1/2–Atg13–FIP200–Atg101 in mammals) and the class III phosphatidylinositol (PtdIns) 3-kinase complex (Atg6–Atg14–Vps15–Vps34 in yeast, and Beclin 1–Atg14(L)–Vps15–Vps34 in mammals) function at upstream nucleation steps, and Atg12–Atg5 and Atg8/LC3–PE (where – indicates covalent attachment) conjugation systems function at downstream elongation steps (Itakura and Mizushima, 2010; Suzuki et al., 2007). On the basis of this hierarchical relationship, we determined the recruitment step of the selective autophagy substrate p62 during canonical autophagy. In contrast to the expectation that p62 is recruited at a late stage through interaction with LC3, we found that a part of p62 can localize to endoplasmic reticulum (ER)-associated autophagosome formation sites independently of core Atg proteins including LC3 (Itakura and Mizushima, 2011). This suggests that LC3 is not the only substrate-recognition molecule.

During our previous mitophagy study, we observed that isolation membranes enclosing mitochondria were tightly associated with rough ER (Yoshii et al., 2011), which is similar to the situation in canonical autophagy (Hayashi-Nishino et al., 2009; Yla-Anttila et al., 2009). This observation suggests that canonical autophagy and mitophagy share similar machinery for the formation of autophagosome or mitophagosome.

In the present study, we first performed hierarchical analysis of mammalian Atg proteins during Parkin-mediated mitophagy and found that structures containing upstream Atg proteins, including the ULK1 complex, can associate with depolarized mitochondria independently of LC3. We further suggest that Atg9, a transmembrane autophagy protein, also targets autophagosome formation sites during canonical autophagy and mitophagy, independent of the ULK1 complex. Thus at least two Atg units, Atg9A and the ULK1 complex, might be independently involved in the initial stages of autophagosome formation, which could be a general mechanism shared by canonical autophagy and selective mitophagy. Autophagosomal LC3 seems to be required for efficient incorporation of damaged mitochondria into the autophagosome at a later stage.

Results

CCCP treatment induces recruitment of upstream Atg proteins to mitochondria

To study Atg protein recruitment to damaged mitochondria, we used mouse embryonic fibroblasts (MEFs) stably expressing exogenous Parkin and the uncoupling reagent carbonyl cyanide m-chlorophenylhydrazone (CCCP), a widely-adopted combination for inducing mitophagy (Narendra et al., 2008). Under normal growing conditions, mitochondria were observed as tubular structures, and only a small number of LC3 puncta, which seldom colocalize with mitochondria, were detected (Fig. 1A). Following CCCP treatment, mitochondria became fragmented and clustered at the perinuclear region, where LC3 puncta also accumulated, as previously reported (Fig. 1A,G) (Narendra et al., 2008).

Because LC3 is present on both complete autophagosomes and elongating isolation membranes, we next determined the presence of Atg16L1, which is specifically present on the isolation membrane, but not on the autophagosome (Mizushima et al., 2010). CCCP treatment induced formation of Atg16L1 puncta around mitochondria, although there were fewer Atg16L1 puncta than LC3 puncta (Fig. 1B,G). These data suggest that most of the LC3 structures represent complete autophagosomes containing mitochondria and that isolation membranes are generated de novo on damaged mitochondria.

Next, we analyzed the recruitment of more upstream Atg factors upon mitophagy induction. Double FYVE-containing protein 1 (DFCP1), a PtdIns(3)*P*-binding protein, is present primarily in the cytoplasm, as well as on the ER and Golgi membranes, and translocates to a subdomain of the ER (termed the omegasome) upon autophagy induction by starvation (Axe et al., 2008). We observed that DFCP1 puncta were also generated around mitochondria following CCCP treatment (Fig. 1C,G). This suggests that the omegasome is also involved in Parkin-mediated mitophagy, which is consistent with our previous electron microscopic analysis showing that ER-associated isolation membranes enclose damaged mitochondria (Yoshii et al., 2011). Another PtdIns(3)*P*-binding protein, WIPI-1, was also recruited to clustered mitochondria in CCCP-treated MEFs (Fig. 1D,G).

Moreover, we detected punctate structures containing Atg14, an autophagy-specific subunit of the class III PtdIns 3-kinase complex (Fig. 1E,G), and ULK1, a subunit of the most upstream autophagy complex (Fig. 1F,G), mostly associated with mitochondria. Live-cell imaging revealed that the ULK1 puncta emerged in close association with mitochondria in CCCP-treated cells, rather than preformed ULK1 puncta moving to the mitochondria from elsewhere (Fig. 1H; supplementary material Movie 1). The colocalization of ULK1 with these mitochondria was transient; the ULK1 structure was detectable for 7.2 ± 2.1 minutes and then disappeared, although the mitochondrial signal persisted. Thus, ULK1 seems to function only at an early stage of mitophagy. Recruitment of these Atg proteins was dependent on Parkin; it was not observed in Parkin-untransfected cells in which Parkin expression is negligible (supplementary material Fig. S1). Taken together, these data suggest that the canonical autophagy machinery is used to produce the isolation membrane on damaged mitochondria in Parkin-mediated mitophagy.

LC3–PE is not required for recruitment of punctate structures containing upstream Atg proteins to damaged mitochondria

Because LC3 functions at a late stage of autophagosome formation (Itakura and Mizushima, 2010), we speculated that localization of the upstream Atg proteins to damaged mitochondria could be independent of LC3. We tested this possibility by using MEFs deficient in Atg3, an E2-like enzyme required for LC3–PE conjugation (Ichimura et al., 2000; Sou et al., 2008). As expected, CCCP-induced degradation of the core 1 subunit of complex III (a mitochondrial inner membrane protein) and disappearance of Mitotracker signals were suppressed in Atg3-knockout (KO) MEFs, suggesting that mitophagy is blocked (supplementary material Fig. S2). Tom20 was degraded both in CCCP-treated wild-type and Atg3 KO MEFs, but it was mediated by the ubiquitin–proteasome system, but not by mitophagy (Chan et al., 2011; Yoshii et al., 2011).

In Atg3 KO cells, GFP–LC3 puncta and the LC3-II form (LC3–PE) were not generated, even after CCCP treatment for 6 hours (Fig. 2A,B). However, Atg16L1 still translocated to mitochondria in CCCP-treated Atg3 KO MEFs (Fig. 2C). Similarly, the punctate structures containing DFCP1 and WIPI-1 were also generated and associated with mitochondria

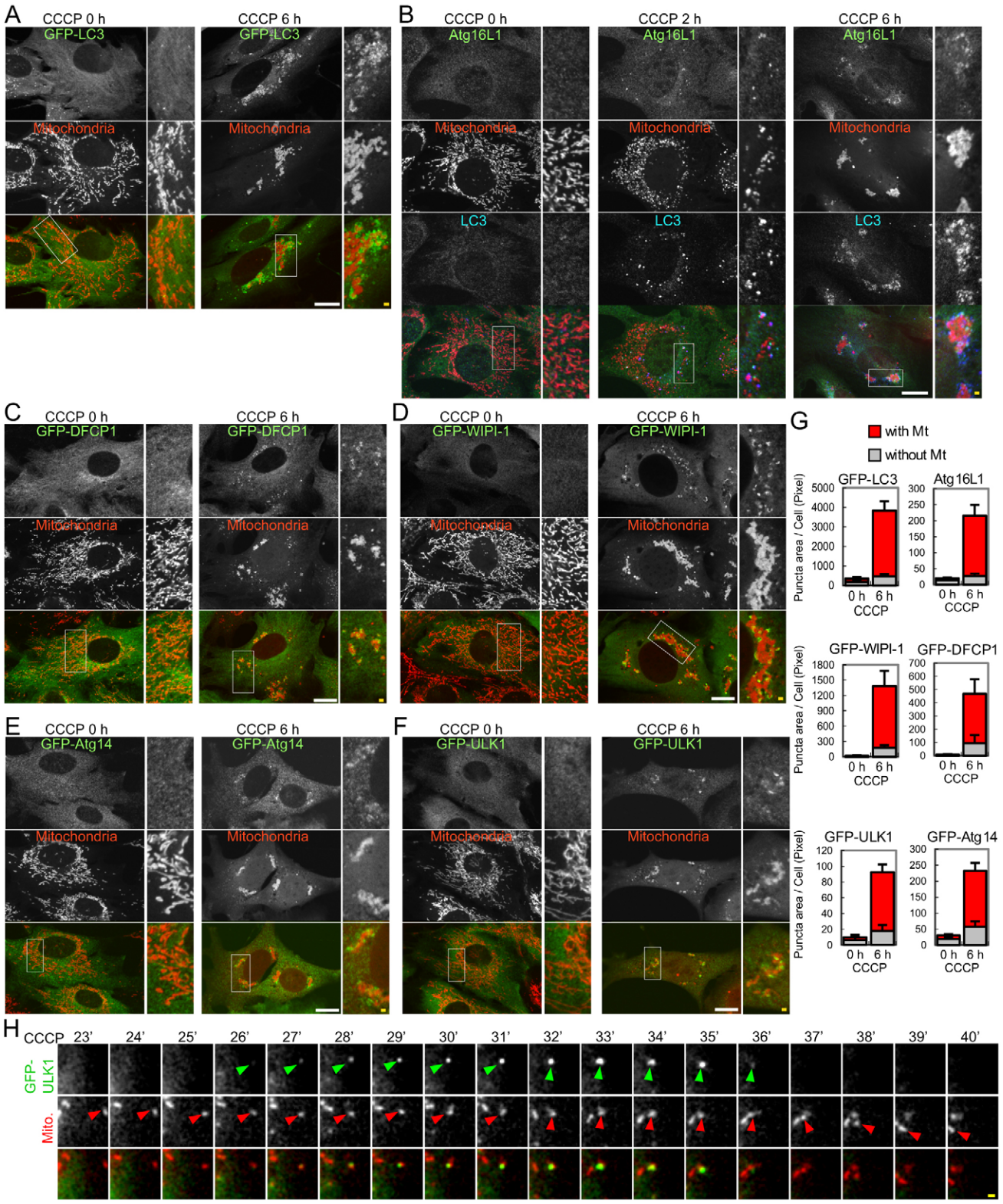

Fig. 1. Upstream Atg proteins are closely associated with damaged mitochondria. Wild-type MEFs stably expressing HA–Parkin (**B**) or co-expressing HA–Parkin with GFP–LC3 (**A**), GFP–DFCP1 (**C**), GFP–WIPI-1 (**D**), GFP–Atg14 (**E**) or GFP–ULK1 (**F**) were pretreated with 50 nM Mitotracker Red CMXRos and then treated with 20 μM CCCP for the indicated periods. Cells were analyzed by immunofluorescence microscopy following staining with antibodies against Atg16L1 (B) or GFP (C–F). (**G**) Quantification of mitochondrial (Mt) association of the Atg punctate structures. Data represent mean ± s.e.m. of 10 cells. (**H**) Selected frames from time-lapse movies of MEFs stably expressing HA–Parkin and GFP–ULK1 following staining with Mitotracker Red CMXRos. The cells were imaged from 23 minutes after the start of CCCP treatment. Localization of GFP–ULK1 and Mitotracker Red are indicated by green and red arrowheads, respectively. See supplementary material Movie 1 for whole images. Signal color is indicated by color of typeface. Scale bars: 10 μm (white) and 1 μm (yellow) (A–F,H).

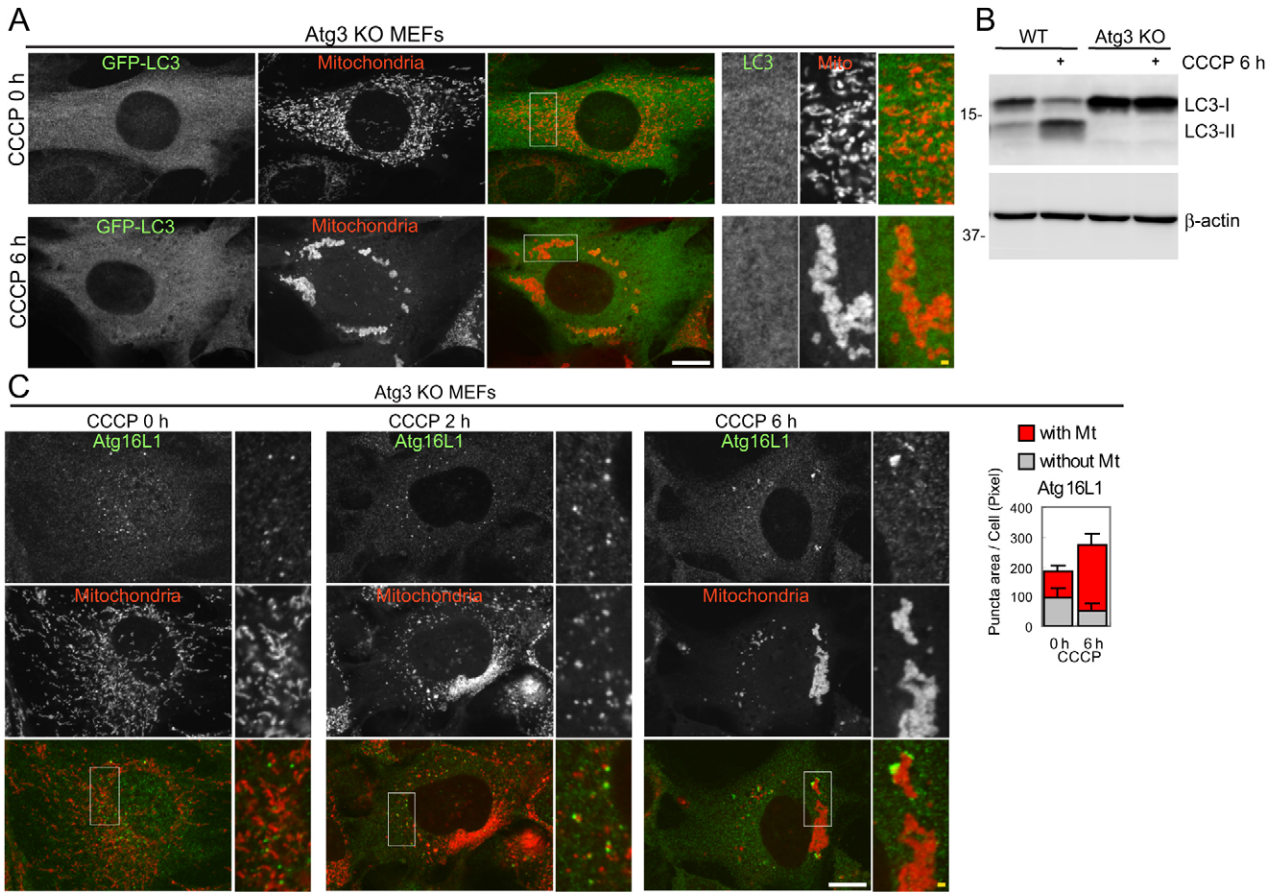

Fig. 2. LC3–PE is not required for recruitment of autophagic structures containing upstream Atg proteins to damaged mitochondria. Atg3 KO MEFs stably expressing HA–Parkin (**B**,**C**) or co-expressing HA–Parkin with GFP–LC3 (**A**) were pretreated with 50 nM Mitotracker Red CMXRos and then treated with 20 μM CCCP for the indicated periods. Cell lysates were analyzed by immunoblot analysis using antibodies against LC3 and β-actin (B). Cells were analyzed by immunofluorescence microscopy following staining with anti-Atg16L1 antibody (C). Quantification of mitochondrial (Mt) association of the Atg16L1 puncta is shown in the right graph (C). Data represent mean ± s.e.m. of 10 cells. Signal color is indicated by color of typeface. Scale bars: 10 μm (white) and 1 μm (yellow) (A,C).

in Atg3 KO cells (supplementary material Fig. S3). These data suggest that membrane-bound LC3 is not required for formation or recruitment of these punctate structures, to which early Atg proteins associate.

FIP200 is required for puncta formation of Atg16L, WIPI-1, Atg14 and ULK1

Having previously reported that the ULK1–FIP200 complex is the most upstream unit among the Atg proteins (Itakura and Mizushima, 2010), we next tested whether FIP200 was required for recruitment of other Atg proteins to damaged mitochondria. Although mitophagy is suppressed in FIP200 KO cells (Yoshii et al., 2011), CCCP-induced mitochondrial clustering was normally observed in FIP200 KO cells (Fig. 3). However, formation of the mitochondria-associated punctate structures of ULK1, Atg14, WIPI-1, Atg5 and Atg16L1 was completely inhibited in FIP200 KO MEFs even after CCCP treatment (Fig. 3, supplementary material Fig. S4). These data suggest that the ULK1–FIP200 complex is the most upstream unit, which is essential for recruitment of PtdIns 3-kinase complex and its effectors in mitophagy. The one exception was that LC3 was still recruited to damaged mitochondria even in FIP200 KO MEFs, which will be discussed below.

Atg9A and the ULK1 complex independently localize to depolarized mitochondria

Atg9 is the only transmembrane protein among the classical Atg proteins required for autophagy (Noda et al., 2000; Saitoh et al., 2009; Young et al., 2006). Yeast Atg9 localizes to the preautophagosomal structure (PAS) and cytoplasmic punctate structures, and mammalian Atg9A localizes to endocytic compartments, the trans-Golgi network and autophagic membranes (Young et al., 2006). In both yeast and mammalian cells, Atg9/Atg9A is known to dynamically shuttle between these organelles (Mari et al., 2010; Young et al., 2006). In yeast, PAS localization of Atg9 is only partially dependent on the Atg1 kinase complex (Suzuki et al., 2007), and Atg1, Atg13 and Atg14 are required for further rearrangement of the Atg9 structures (Mari et al., 2010).

We investigated whether Atg9A is involved in Parkin-mediated mitophagy. In Atg9A KO MEFs, degradation of the core 1 subunit of complex III (supplementary material Fig. S2A), and disappearance of Mitotracker signals (supplementary material

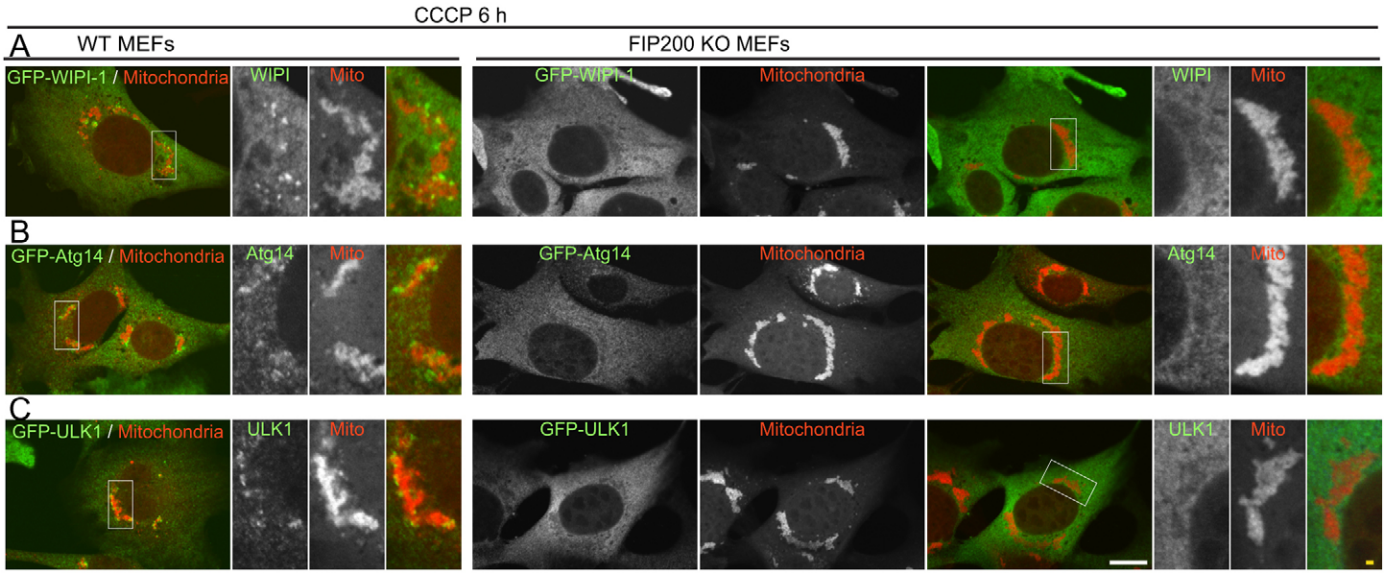

Fig. 3. FIP200 is required for puncta formation of WIPI-1, Atg14 and ULK1. Wild-type and FIP200 KO MEFs stably co-expressing HA–Parkin with GFP–WIPI-1 (**A**), GFP–Atg14 (**B**), or GFP–ULK1 (**C**) were pre-treated with 50 nM Mitotracker Red CMXRos and then treated with 20 μM CCCP for an additional 6 hours. Cells were analyzed by immunofluorescence microscopy using anti-GFP (A–C) antibodies. Signal color is indicated by color of typeface. Scale bars: 10 μm (white) and 1 μm (yellow).

Fig. S2B) were markedly delayed, confirming that Atg9A is required for mitophagy. Formation of isolation membrane/autophagosomes was in fact suppressed in Atg9A KO MEFs; mitochondria with partially ruptured outer membranes accumulate as we previously observed in FIP200 KO MEFs (Yoshii et al., 2011) (supplementary material Fig. S2C). We generated an antibody against mouse Atg9A and confirmed its specificity using Atg9A KO MEFs (supplementary material Fig. S5). Under growing conditions, numerous small Atg9A puncta were observed throughout the cytoplasm and in the perinuclear region, which is likely to represent the Golgi complex, as previously reported (Young et al., 2006) (Fig. 4A, also see below). In CCCP-treated Parkin-expressing MEFs, many small Atg9A puncta gathered at the perinuclear region, and associated closely with clustered mitochondria (Fig. 4A). Translocation of the Atg9A structures was also observed in FIP200 KO cells, suggesting that it is independent of the ULK1–FIP200 complex (Fig. 4B). When visualized by electron microscopy, small vesicles were occasionally observed around clustered mitochondria both in wild-type and FIP200 KO MEFs (Fig. 4C). The Atg9A signals were detected on or close to isolation membranes in wild-type MEFs and around mitochondria in FIP200 KO MEFs by immunoelectron microscopy (Fig. 4C). Some of the Atg9A signals formed a circular shape (Fig. 4Cg, arrow), suggesting that Atg9A-containing vesicles are recruited.

We then analyzed the requirement of Atg9A for the recruitment of other Atg proteins to mitochondria. ULK1 puncta accumulated in Atg9A KO cells, but they were not significantly colocalized with mitochondria in cells that had not been treated with CCCP (Fig. 5A). However, as in wild-type cells, these ULK1 puncta became associated with mitochondria following CCCP treatment (Fig. 5A). The total area of the ULK1 puncta associating with mitochondria was higher in Atg9A KO MEFs (~460 pixels/cell) (Fig. 5A) than in wild-type MEFs (~75 pixels/cell) (Fig. 1G), suggesting that Atg9A is required for ULK1 retrieval from mitochondria. Recruitment of ULK1 to clustered mitochondria in the absence of Atg9A was also observed by immunoelectron microscopy (supplementary material Fig. S6A). Recruitment of Atg14, WIPI-1, Atg5 and Atg16L1 to damaged mitochondria was completely abolished in Atg9A KO cells (Fig. 5B, supplementary material Fig. S4). However, LC3 still translocated to mitochondria following CCCP treatment in Atg9A KO MEFs, as well as in FIP200 KO MEFs (Fig. 6A). The LC3-II form was also generated in these cells (Fig. 6B). Thus, Atg9A and ULK1 independently localize to damaged mitochondria, and both are essential for the subsequent organization of mitophagosomes, but not for recruitment of LC3.

Consistent with these observations, Atg9A and ULK1 did not completely colocalize (Fig. 5C). GFP–ULK1 puncta appeared to associate with mitochondria more closely than the Atg9A structures. By contrast, ULK1 colocalized with the typical isolation membrane marker Atg16L1 (Fig. 5C). These results suggest that the functional stage and site of the ULK1–FIP200 complex and Atg9A are different.

Atg9A and the ULK1 complex independently localize to the autophagosome formation site during starvation-induced autophagy

Because the hierarchical position of Atg9A in starvation-induced canonical autophagy has not yet been systematically evaluated in mammalian cells, we investigated it by methods we used previously for other Atg proteins (Itakura and Mizushima, 2010). Under starvation conditions, only a small number of Atg9A puncta colocalized with ULK1. However, the colocalization rate was greatly increased in cells treated with wortmannin; almost all ULK1 puncta became positive for Atg9A (Fig. 7A). These data suggest that Atg9A is transiently present at the autophagosome formation site and rapidly dissociates in a PtdIns-3-kinase-dependent manner.

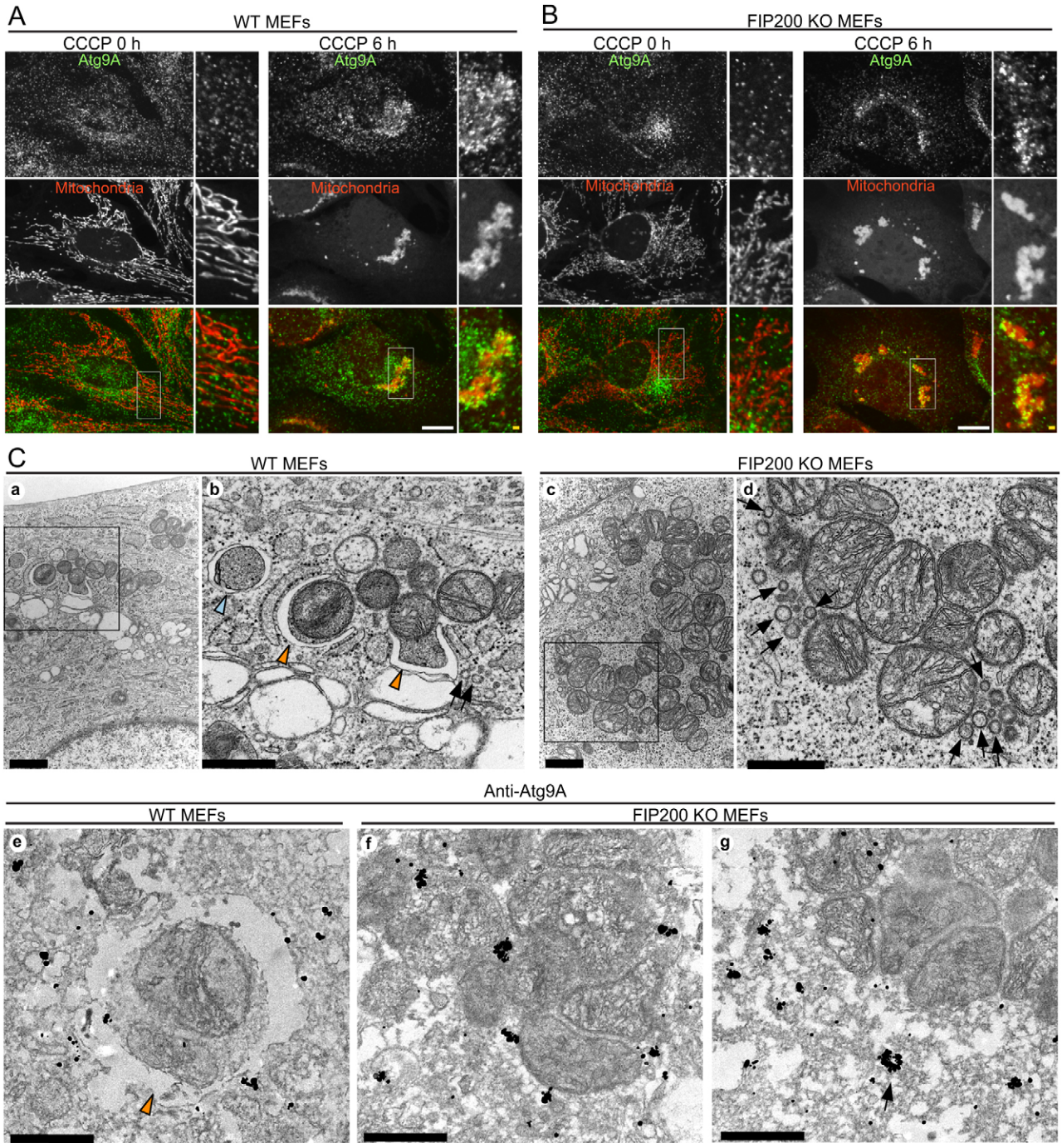

Fig. 4. Atg9A recruitment to damaged mitochondria is independent of FIP200. (**A**,**B**) Wild-type (A) and FIP200 KO MEFs (B) stably expressing HA–Parkin were pretreated with 50 nM Mitotracker Red CMXRos and then treated with 20 μM CCCP for 6 hours. Cells were analyzed by immunofluorescence microscopy using anti-Atg9A antibody. Signal color is indicated by color of typeface. Scale bars: 10 μm (white) and 1 μm (yellow). (**C**) Wild-type (a,b,e) and FIP200 KO (c,d,f,g) MEFs stably expressing HA–Parkin were treated with 20 μM CCCP for 6 hours and analyzed by conventional electron microscopy (a–d) or immunoelectron microscopy using anti-Atg9A antibody (e–g). Arrows indicate small vesicles accumulating around clustered mitochondria. Orange and blue arrowheads indicate autophagic structures containing/enclosing and not containing/enclosing mitochondria, respectively. Scale bars: 1 μm (a,c), 500 nm (b,d,e,f,g).

We next determined whether Atg9A recruitment is dependent on the ULK1–FIP200 complex using p62 as a marker for the autophagosome formation site (Itakura and Mizushima, 2011). Although we observed only partial colocalization between Atg9A and p62 in wild-type cells, Atg9A was detected on almost all p62-positive structures in FIP200 KO cells (Fig. 7B), which should represent the autophagosome formation sites (Itakura and Mizushima, 2011). Immunoelectron microscopy revealed that p62-positive amorphous structures were associated with vesicle-like membranes, which might represent Atg9A-containing vesicles accumulating at the autophagosome formation site (supplementary material Fig. S6B). Thus, recruitment of

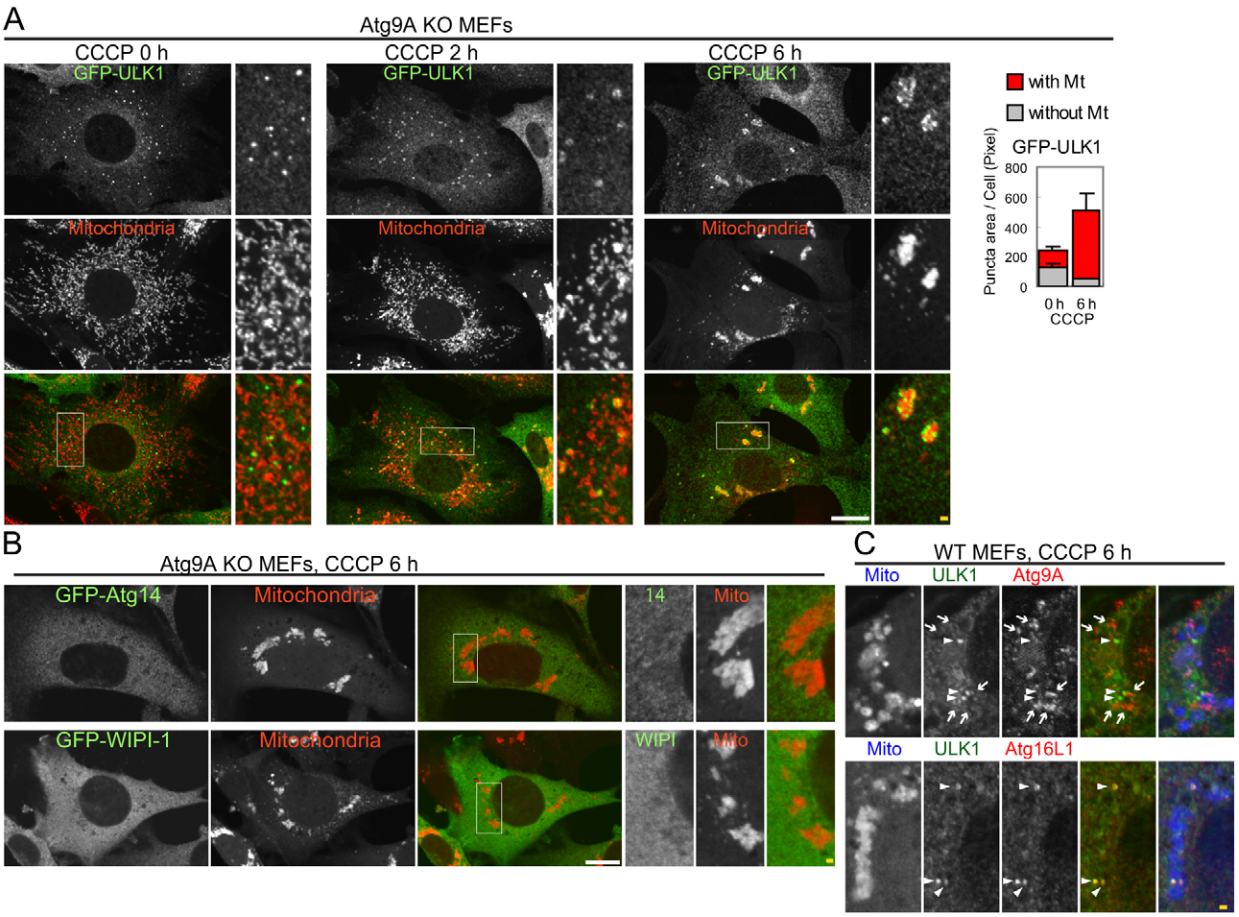

Fig. 5. The ULK1 punctate structure is recruited to damaged mitochondria in an Atg9-independent manner. (**A**,**B**) Atg9A KO MEFs stably co-expressing HA–Parkin with GFP–ULK1 (A), or GFP–Atg14 or GFP–WIPI-1 (B) were pretreated with 50 nM Mitotracker Red CMXRos and then treated with 20 μM CCCP for the indicated periods. Cells were analyzed by immunofluorescence microscopy using anti-GFP antibody. Quantification of mitochondrial (Mt) association of the ULK1 puncta in Atg9KO MEFs is shown in the right graph (A). Data represent mean ± s.e.m. of 10 cells. (**C**) ULK1 does not colocalize with Atg9A. GFP–ULK1-expressing MEFs were treated as in A, and stained with anti-Atg9A or anti-Atg16L1 antibodies. The ULK1-positive and Atg9A-positive puncta are indicated by arrowheads and arrows, respectively. Signal color is indicated by color of typeface. Scale bars: 10 μm (white) and 1 μm (yellow) (A–C).

Atg9A-containing structures does not require FIP200. These data also suggest that Atg9A recycling requires FIP200, as well as ULK1 (Young et al., 2006).

These observations suggest that Atg9A might be the most upstream factor among mammalian Atg proteins. However, formation of ULK1 puncta was not affected in Atg9A KO MEFs; instead, as shown in Fig. 5A, ULK1 puncta accumulated in even non-starved cells, whereas ULK1 puncta formation was suppressed in FIP200 KO MEFs as we have previously reported (Hara et al., 2008) (Fig. 7C). Starvation-induced puncta formation of Atg14 and WIPI-1 was blocked in Atg9A KO MEFs, as well as in FIP200 KO MEFs (Fig. 7C). These data suggest that, as observed in Parkin-mediated mitophagy, Atg9A and the ULK1 complex independently localize to the autophagosome formation site, and both are required for recruitment of downstream factors such as Atg14 and WIPI-1.

LC3–PE is important for efficient incorporation of mitochondria inside autophagosomes

Finally, we analyzed the role of autophagosomal LC3 in mitophagy by electron microscopy using Atg3 KO MEFs. In wild-type cells, approximately 40% of autophagosomes contained mitochondria at 6 hours following CCCP treatment (Fig. 8Aa,B). A previous study showed that partially elongated, but not completely closed, isolation membranes can be generated in Atg3 KO MEFs (Sou et al., 2008). Indeed, isolation membranes and autophagosome-like structures were observed during mitophagy in Atg3 KO MEFs (Fig. 8Ab). This is consistent with our observation that isolation membrane markers were detected in close proximity to mitochondria in Atg3 KO MEFs (Fig. 2C, supplementary material Fig. S3). However, these autophagosome-like structures failed to enclose mitochondria even though they were generated next to mitochondria (Fig. 8B). These data suggest that autophagosomal LC3 is important for efficient incorporation of damaged mitochondria into the autophagosome.

Discussion

We have demonstrated how Atg proteins are recruited to damaged mitochondria. It has been proposed that damaged mitochondria are recognized by the isolation membrane through the interaction between autophagosomal LC3 and a mitochondrial adaptor protein such as p62 or Nix (Johansen and Lamark, 2011; Kirkin et al., 2009; Youle and Narendra, 2011).

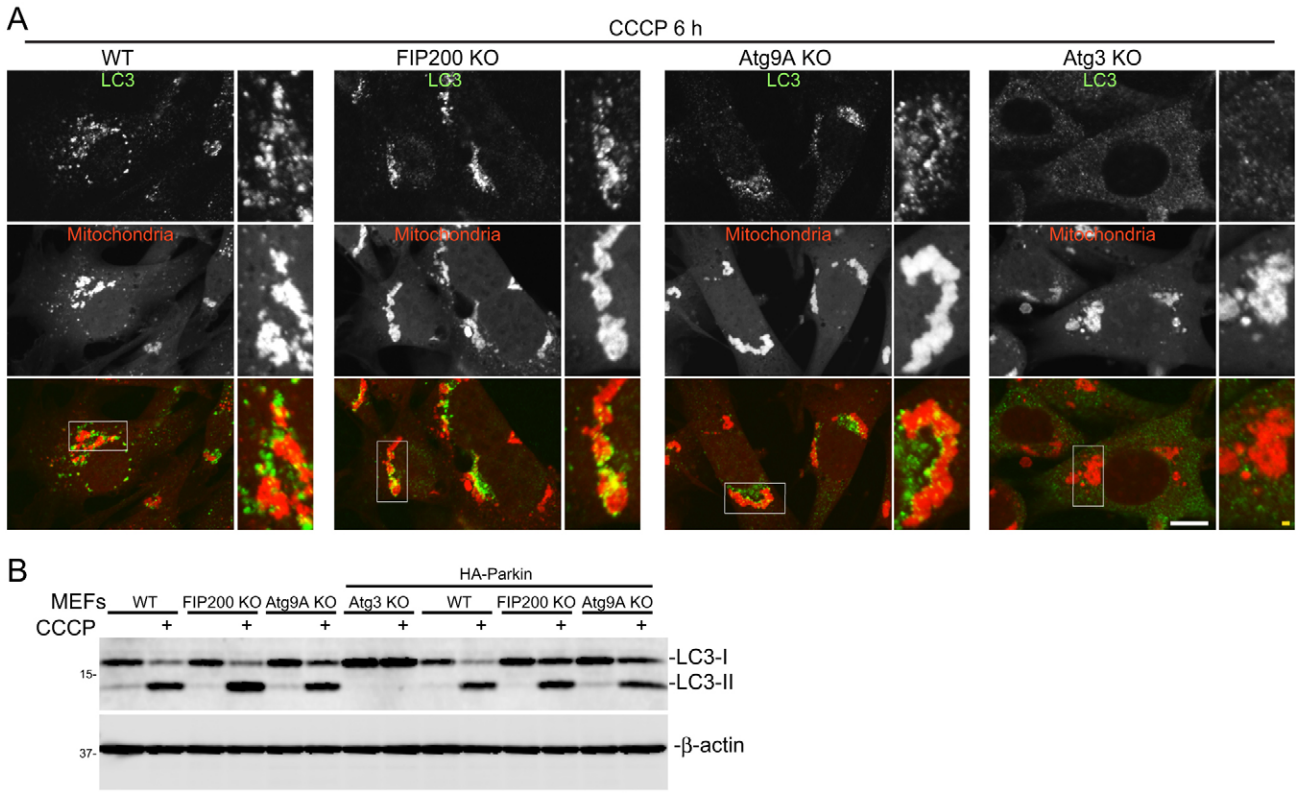

Fig. 6. Recruitment of LC3 to depolarized mitochondria is suppressed in Atg3 KO MEFs but not in FIP200 KO and Atg9A KO MEFs. Wild-type, FIP200 KO, Atg9A KO and Atg3 KO MEFs stably expressing HA–Parkin were pretreated with 50 nM Mitotracker Red CMXRos and then treated with 20 μM CCCP for 6 hours (**A**) or 24 hours (**B**). Cells were analyzed by immunofluorescence microscopy using anti-LC3 antibody (A), and by immunoblot analysis using antibodies against LC3 and β-actin (B). Signal color is indicated by color of typeface. Scale bars: 10 μm (white) and 1 μm (yellow) (A).

However, in the present study, we showed that the interaction between LC3 and the adaptor molecules is not the first recognition step of mitophagy. On the basis of our results, we propose the following model (Fig. 8C). Upon mitochondrial depolarization by CCCP, Parkin is recruited to the mitochondrial membrane, which induces formation of transient ULK1 puncta in close association with the mitochondria. Parkin also induces recruitment of the Atg9A structures. Mitochondrial targeting of these two structures is not interdependent, but both are essential for recruitment of the downstream class III PtdIns 3-kinase complex and its effectors. These findings suggest that the mitophagosome is generated de novo on damaged mitochondria. LC3–PE is important for efficient incorporation of damaged mitochondria inside autophagosomes at a later step.

We also determined the hierarchical position of Atg9A in canonical starvation-induced autophagy induction, and found that it is similar to that in mitophagy; Atg9A and FIP200 independently localize to the autophagosome formation site, which is labeled with p62 (Fig. 7). Very recently, a similar finding was also reported in autophagy against *Salmonella* (xenophagy), where ULK1 and Atg9A independently localize to the *Salmonella*-containing vacuoles (SCVs) (Kageyama et al., 2011).

Although the hierarchical position of mammalian Atg9A is similar to that of yeast Atg9, there is a slight difference. In yeast, Atg9 markedly accumulates at the PAS in Δ*atg1* and Δ*atg13* cells, but less so in Δ*atg17* cells (Reggiori et al., 2004; Suzuki et al., 2007). There is no Atg17 homolog in mammals, and FIP200 is proposed to be a functional counterpart (Hara et al., 2008). However, Atg9A localization to the autophagosome formation site in canonical autophagy (Fig. 7), mitophagy (Fig. 4) and *Salmonella* xenophagy (Kageyama et al., 2011) is not affected by deletion of FIP200. Furthermore, mammals have additional regulatory factors such as p38IP for Atg9A translocation (Webber and Tooze, 2010a).

Recruitment of downstream Atg proteins to the autophagosome formation site is somewhat complicated. We have reported that recruitment of LC3, Atg16L1, WIPI-1 and DFCP1 to the autophagosome formation site is dependent on PtdIns 3-kinase and FIP200 in starvation-induced canonical autophagy (Itakura and Mizushima, 2010). However, Kageyama and colleagues recently reported that recruitment of WIPI-1 and DFCP1, but not of LC3 and Atg5, to SCVs is dependent on PtdIns 3-kinase, FIP200 and Atg9A (Kageyama et al., 2011). In addition, Kim and co-workers reported that wortmannin treatment does not inhibit LC3 recruitment to photodamage-induced mitophagosomes (Kim et al., 2007). We also observed that LC3 can be recruited to CCCP-induced depolarized mitochondria even in FIP200 KO MEFs and Atg9A KO MEFs (Fig. 6). Thus, the mechanism of LC3 recruitment seems to be different between canonical autophagy and mitophagy or xenophagy. Although mitophagy and xenophagy might share a similar mechanism, one discrepancy is that we could detect neither Atg5 nor Atg16L1 on mitochondria (supplementary

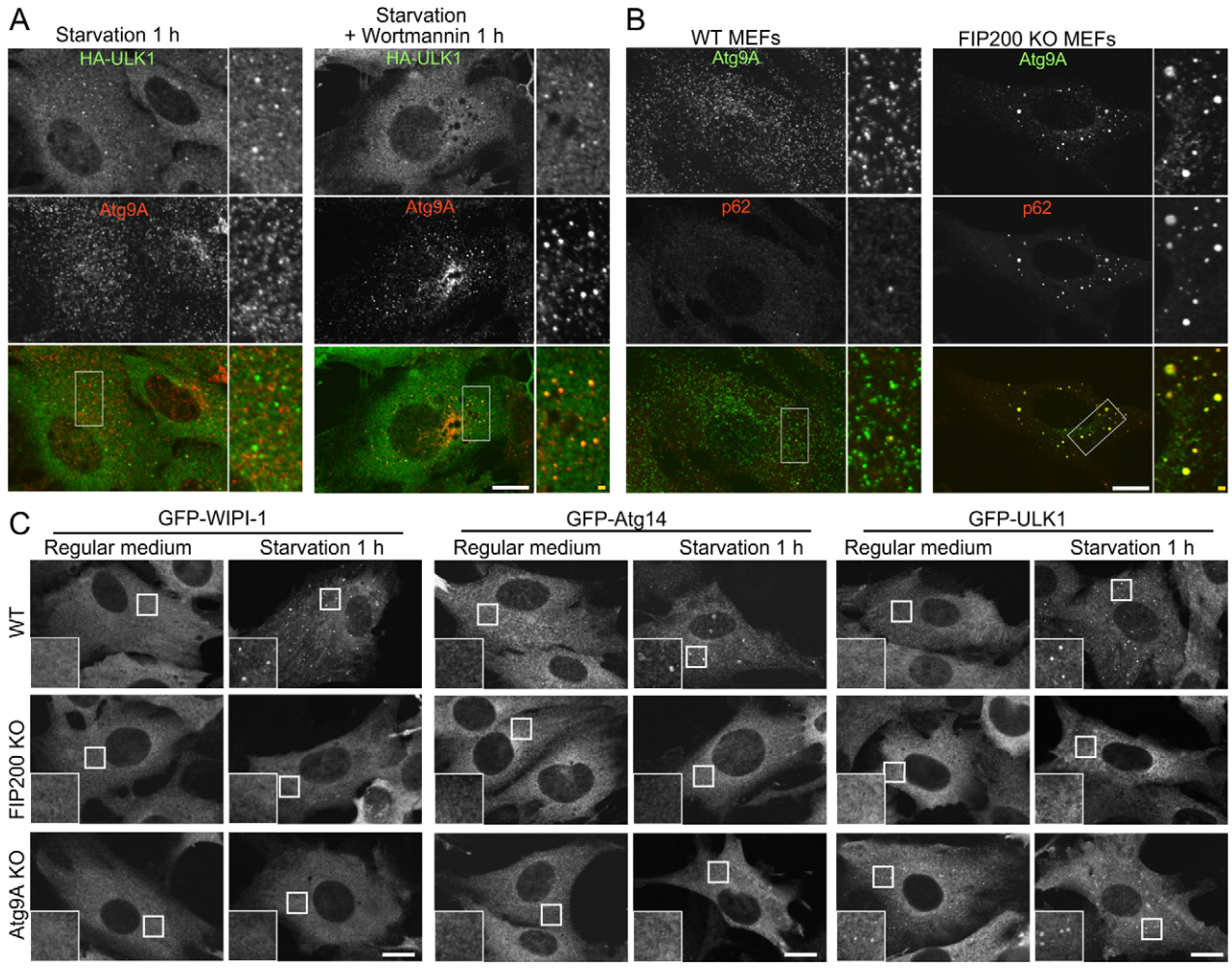

Fig. 7. Atg9A and the ULK1 complex independently localize to the autophagosome formation site during starvation-induced autophagy. (**A**) Wild-type MEFs stably expressing HA–ULK1 were cultured in starvation medium in the presence or absence of 200 nM wortmannin for 1 hour and analyzed by immunofluorescence microscopy using anti-HA and anti-Atg9A antibodies. (**B**) Wild-type and FIP200 KO MEFs were analyzed by immunofluorescence microscopy using anti-Atg9A and anti-p62 antibodies. (**C**) Wild-type, Atg9A KO or FIP200 KO MEFs stably expressing GFP–WIPI-1, GFP–Atg14 or GFP–ULK1 were cultured in regular or starvation medium for 1 hour. Cells were subjected to immunofluorescence microscopy using anti-GFP antibody. Signal color is indicated by color of typeface. Scale bars: 10 µm (white) and 1 µm (yellow) (A–C).

material Fig. S4). This was unexpected because Atg5 and Atg16L1 are important for lipidation and localization of LC3 (Fujita et al., 2008; Mizushima et al., 2001). Undetectable levels of Atg5 and Atg16L1 might be sufficient for LC3 recruitment, or LC3 might be lipidated elsewhere. How CCCP induces LC3 lipidation needs to be investigated in the future.

In yeast, retrograde transport of Atg9 from the PAS to the peripheral pools requires Atg1, Atg13, Atg2 and Atg18 (Reggiori et al., 2004). The Atg9 compartment might provide an initial membrane source, which is further rearranged by the functions of Atg1, Atg13 and PtdIns(3)*P* (Mari et al., 2010). In mammals, although starvation-dependent trafficking of mammalian Atg9A from the trans-Golgi network to endosomes requires ULK1, mAtg13, and PtdIns 3-kinase activity (Chan et al., 2009; Tang et al., 2011; Young et al., 2006), it has not been determined whether these factors are also required for retrograde transport of Atg9A from the autophagosome formation site. Here, we showed that Atg9A recycling requires both FIP200 and PtdIns 3-kinase activity in canonical autophagy. Because the colocalization of ULK1 and Atg9A was clarified only after wortmannin treatment, most Atg9A structures should rapidly dissociate from the autophagosome formation site. Atg9A-containing vesicles might dissociate from the autophagosome formation site once sufficient PtdIns(3)*P* is generated.

To which structures do these Atg proteins localize during mitophagy? It was suggested that Atg14 functions on the ER in canonical autophagy in mammalian cells (Matsunaga et al., 2010). Because typical ER-associated isolation membranes are generated during Parkin-mediated mitophagy (Yoshii et al., 2011), we speculate that the ULK1 and Atg14 complexes are transiently present on these isolation membranes and/or the associated ER. This idea could be supported by our observation that ULK1 colocalizes with Atg16L1, an isolation membrane marker (Fig. 5C). Whether the ER and mitochondria association occurs before recruitment of Atg proteins is an important question that needs to be resolved.

By contrast, the nature of the Atg9A structure is unknown. It is widely believed that Atg9/Atg9A can translocate on small

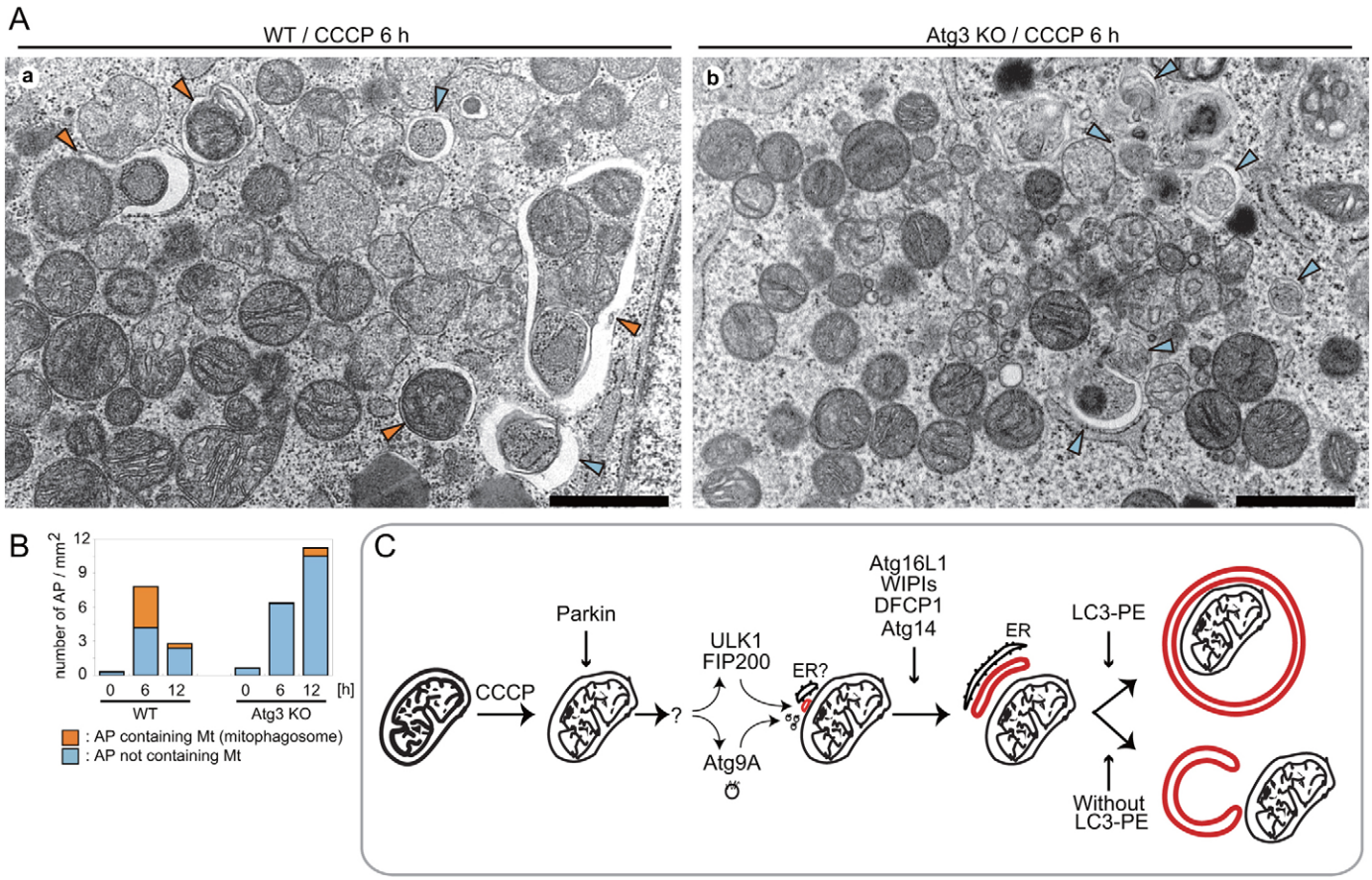

Fig. 8. Autophagosomal LC3 is important for incorporation of mitochondria into the autophagosome. (**A**) Wild-type (a) and Atg3 KO MEFs (b) stably expressing HA–Parkin were treated with 20 μM CCCP for 6 hours. Orange and blue arrowheads indicate autophagic structures containing or enclosing and not containing or enclosing mitochondria, respectively. Scale bars: 1 μm. (**B**) The number of autophagosomes (AP) containing or enclosing and not containing or enclosing mitochondria (Mt) were counted from at least 20 randomly selected areas in wild-type and Atg3 KO MEFs at indicated time points following CCCP treatment. (**C**) Model of recruitment of Atg factors to depolarized mitochondria in Parkin-mediated mitophagy. Parkin translocates to depolarized mitochondria, and induces formation of the ULK1 puncta on mitochondria. This structure represents the 'mitophagosome formation site'. The endoplasmic reticulum is probably involved in this process. Independent of the recruitment of the ULK1 complex, Atg9A, which is probably contained in vesicles, also translocates to these mitochondria. Both the ULK1 complex and Atg9A are required for subsequent puncta formation of Atg14, WIPIs, DFCP1 and Atg16L1, and organization of mitophagosomes (red). LC3 can be recruited independent of Atg9A and FIP200. Autophagosomal LC3—PE is important for efficient incorporation of damaged mitochondria into the autophagosome.

vesicles (Webber and Tooze, 2010b). Our electron microscopy studies also suggest that vesicles containing Atg9A are involved in mitophagy (Fig. 4C). These vesicles might fuse directly with the isolation membrane or they might exchange some components (lipids or proteins) with the isolation membrane. Because the localization of Atg9A and ULK1 is not exactly the same (Fig. 5C), Atg9A structures might be involved in isolation membrane formation without direct fusion. This idea could explain the retrograde translocation of Atg9A from mitochondria; otherwise it would be difficult to imagine that the transmembrane protein could be extracted from the isolation membrane. Further analyses will be required to elucidate the precise role of Atg9A in both canonical autophagy and Parkin-dependent mitophagy. Finally, the mechanism underlying specific recognition of depolarized mitochondria is also unknown. We have shown that the binding between LC3 and its adaptors is not essential for this recognition step, therefore it will be important to investigate targeting mechanism of ULK1- and Atg9A-containing structures.

Materials and Methods

Cell culture and transfection

MEFs were cultured in Dulbecco's modified Eagle's medium (DMEM) supplemented with 10% fetal bovine serum, 50 μg/ml penicillin and streptomycin (regular medium) in a 5% CO_2 incubator. Atg3 KO (Sou et al., 2008), FIP200 KO (Gan et al., 2006) and Atg9A KO (Saitoh et al., 2009) MEFs were generated previously. For starvation treatment, cells were washed with phosphate-buffered saline (PBS) and incubated in amino-acid-free DMEM without serum (starvation medium). Wortmannin, puromycin, and CCCP were purchased from Sigma (St Louis, MO). Mitotracker Red CMXRos was purchased from Invitrogen (Carlsbad, CA).

Plasmids

The following plasmids have been previously described: pMXs-IP GFP-LC3 (Hara et al., 2008), pMRX-IP GFP-ULK1, pMXs-puro GFP-DFCP1, pMXs-puro GFP-WIPI-1, pMXs-IP GFP-Atg14 (Itakura and Mizushima, 2010) and pMXs-IP HA-Parkin (Yoshii et al., 2011).

Retroviral infection and generation of stable cell lines

Stable cell lines were generated using a retroviral expression system as previously described (Hara et al., 2008; Kitamura et al., 2003). Briefly, Plat E cells (kindly provided by Toshio Kitamura, University of Tokyo, Tokyo, Japan) were

transiently transfected with pMXs vectors using FuGENE 6 reagent (Roche Applied Science, Mannheim, Germany). After culture for 72 hours, the growth medium containing retrovirus was collected. MEFs were incubated with the collected virus-containing medium with 8 μg/ml polybrene for 24 hours. Uninfected cells were removed by puromycin selection.

Antibodies

To generate antibodies against mouse Atg9A, mouse Atg9A cDNA (amino acid residues 506–839) was subcloned into pGEX-6p-1 (GE Healthcare, Little Chalfont, UK). The resultant glutathione-*S*-transferase-fused Atg9A was used to immunize rabbits. Antisera were affinity purified. Rat monoclonal anti-green fluorescent protein (GFP) antibodies (GF090R) were purchased from Nacalai Tesque (Kyoto, Japan). Guinea-pig polyclonal anti-p62 antibodies were purchased from Progen (Heidelberg, Germany). The rabbit polyclonal antibodies against LC3 (LC3#1) for immunoblotting (Hosokawa et al., 2006) and Atg16L1 (Mizushima et al., 2003) have been described previously. Mouse monoclonal anti-LC3 antibodies (Clone LC3 1703) for immunofluorescence were purchased from COSMO BIO (Tokyo, Japan). Mouse monoclonal anti-HA (16B12) antibodies were purchased from Covance Research Products.

Immunocytochemistry

Cells grown on coverslips were washed with PBS and fixed in 4% paraformaldehyde in PBS for 10 minutes at 4℃. For mitochondrial staining, cells were pretreated with 50 nM Mitotracker Red CMXRos for at least 15 minutes before treatment with 20 μM CCCP (in the presence of Mitotracker Red CMXRos). Fixed cells were permeabilized with 50 μg/ml digitonin in PBS for 5 minutes, blocked with 3% bovine serum albumin in PBS for 30 minutes, and incubated with primary antibodies for 1 hour. After washing, cells were incubated with Alexa-Fluor-488-conjugated goat anti-rat, anti-rabbit or anti-mouse IgG, Alexa-Fluor-564-conjugated goat anti-rabbit or anti-guinea pig IgG, or Alexa-Fluor-660-conjugated goat anti-rabbit IgG secondary antibodies (Invitrogen) for 30 minutes. Images were acquired on a confocal laser microscope (FV1000D IX81, Olympus, Tokyo, Japan) using a 60× 1.42 numerical aperture (NA) oil-immersion objective lens with a 1.5× zoom factor and captured into Fluoview software (Olympus). The image size was set at 1024×1024 pixels.

Live-cell imaging

Live-cell fluorescence imaging was performed with a microscope (IX81), Olympus 60× PlanAPO oil-immersion lens (NA 1.42) and a CCD camera (CoolSNAP HQ^2, Photometrics, Tucson, AZ). Cells expressing GFP–ULK1 were placed on a glass-bottomed dish 2 days before observation. Mitotracker Red CMXRos (10 nM) was added for 30 minutes, followed by 20 μM CCCP. During live imaging, the culture dish was mounted in a chamber (TOKAI HIT, Shizuoka, Japan) to maintain incubation conditions at 37℃ and 5% CO_2. GFP and Mitotracker were illuminated with a 100 W mercury arc lamp attenuated 12% by a neutral-density filter, and two-color time-lapse images were acquired with 500 msecond (GFP) or 20 msecond (Mitotracker) exposure time at 30 second intervals. The external devices (shutters, filter wheels, stage and camera) were controlled and image data were processed by MetaMorph version 7.0 (Molecular Devices Japan, Tokyo, Japan).

Quantification of mitochondrial association of punctate structures

To quantify mitochondrial association of punctate structures of Atg proteins, immunofluorescence images were processed with morphology filters provided by MetaMorph as outlined in (supplementary material Fig. S7). First, cytoplasmic background images were created by applying a close-open filter to the each Atg protein and mitochondria images, respectively. The background signals were subtracted from the original images, and then the resultant images were binarized to create images of the total Atg protein signals and total mitochondria signals. The Atg signals contacting mitochondria were extracted from the total Atg signals with a reconstruction filter using the total mitochondrial signals. Total pixel area of Atg puncta containing and not containing mitochondria was measured from the binary images.

Electron microscopy

MEFs were cultured on collagen-coated plastic coverslips. They were fixed in 2.5% glutaraldehyde in 0.1 M sodium phosphate buffer, pH 7.4, for 2 hours. The cells were washed in the same buffer three times, post-fixed in 1% osmium tetroxide in 0.1 M phosphate buffer for 1 hour, dehydrated and embedded in Epon 812 according to a standard procedure (Hara et al. 2008). Ultrathin sections were stained with uranyl acetate and lead citrate, and observed under a Hitach H-7100 electron microscope.

For immunoelectron microscopy analysis, cells were fixed with 4% paraformaldehyde in 0.1 M sodium phosphate buffer, pH 7.4, for 2 hours at room temperature. The pre-embedding silver enhancement immunogold method was performed as previously described (Yoshimori et al., 2000).

Immunoblotting

Immunoblotting was performed as previously described (Itakura et al., 2008).

Acknowledgements

We thank Masaaki Komatsu (Tokyo Metropolitan Institute of Medical Science) for providing Atg3 KO MEFs, Jun-Lin Guan (University of Michigan) for FIP200 KO MEFs, Tatsuya Saitoh and Shizuo Akira (Osaka University) for Atg9A KO MEFs, and Toshio Kitamura (The University of Tokyo) and Shoji Yamaoka (Tokyo Medical and Dental University) for the retroviral vectors and Plat-E cells. We also thank Naotada Ishihara and Atsushi Tanaka for critical reading of this manuscript and helpful discussions.

Funding

This work was supported by the Funding Program for Next Generation World-Leading Researchers and Grants-in-Aid for Scientific Research from the Ministry of Education, Culture, Sports, Science and Technology, Japan (to N.M.), and grants for a research fellowship of the Japan Society for the Promotion of Science for Young Scientists (to E.I. and I.K.-H.).

Supplementary material available online at
http://jcs.biologists.org/lookup/suppl/doi:10.1242/jcs.094110/-/DC1

References

Axe, E. L., Walker, S. A., Manifava, M., Chandra, P., Roderick, H. L., Habermann, A., Griffiths, G. and Ktistakis, N. T. (2008). Autophagosome formation from membrane compartments enriched in phosphatidylinositol 3-phosphate and dynamically connected to the endoplasmic reticulum. *J. Cell Biol.* **182**, 685-701.

Chan, E. Y. W., Longatti, A., McKnight, N. C. and Tooze, S. A. (2009). Kinase-inactivated ULK proteins inhibit autophagy via their conserved C-terminal domain using an Atg13-independent mechanism. *Mol. Cell. Biol.* **29**, 157-171.

Chan, N. C., Salazar, A. M., Pham, A. H., Sweredoski, M. J., Kolawa, N. J., Graham, R. L., Hess, S. and Chan, D. C. (2011). Broad activation of the ubiquitin-proteasome system by Parkin is critical for mitophagy. *Hum. Mol. Genet.* **20**, 1726-1737.

Chen, D., Gao, F., Li, B., Wang, H., Xu, Y., Zhu, C. and Wang, G. (2010). Parkin mono-ubiquitinates BCL-2 and regulates autophagy. *J. Biol. Chem.* **285**, 38214-38223.

Ding, W. X., Ni, H. M., Li, M., Liao, Y., Chen, X., Stolz, D. B., Dorn, G. W., II and Yin, X. M. (2010). Nix is critical to two distinct phases of mitophagy: reactive oxygen species (ROS)-mediated autophagy induction and Parkin-ubiqutin-p62-mediated mitochondria priming. *J. Biol. Chem.* **285**, 27879-27890.

Fujita, N., Itoh, T., Omori, H., Fukuda, M., Noda, T. and Yoshimori, T. (2008). The Atg16L complex specifies the site of LC3 lipidation for membrane biogenesis in autophagy. *Mol. Biol. Cell* **19**, 2092-2100.

Gan, B., Peng, X., Nagy, T., Alcaraz, A., Gu, H. and Guan, J. L. (2006). Role of FIP200 in cardiac and liver development and its regulation of TNFα and TSC-mTOR signaling pathways. *J. Cell Biol.* **175**, 121-133.

Gegg, M. E., Cooper, J. M., Chau, K. Y., Rojo, M., Schapira, A. H. and Taanman, J. W. (2010). Mitofusin-1 and Mitofusin-2 are ubiquitinated in a PINK1/parkin dependent manner upon induction of mitophagy. *Hum. Mol. Genet.* **19**, 4861-4870.

Geisler, S., Holmstrom, K. M., Skujat, D., Fiesel, F. C., Rothfuss, O. C., Kahle, P. J. and Springer, W. (2010). PINK1/Parkin-mediated mitophagy is dependent on VDAC1 and p62/SQSTM1. *Nat. Cell Biol.* **12**, 119-131.

Hara, T., Takamura, A., Kishi, C., Iemura, S., Natsume, T., Guan, J. L. and Mizushima, N. (2008). FIP200, a ULK-interacting protein, is required for autophagosome formation in mammalian cells. *J. Cell Biol.* **181**, 497-510.

Hayashi-Nishino, M., Fujita, N., Noda, T., Yamaguchi, A., Yoshimori, T. and Yamamoto, A. (2009). A subdomain of the endoplasmic reticulum forms a cradle for autophagosome formation. *Nat. Cell Biol.* **11**, 1433-1437.

Hosokawa, N., Hara, Y. and Mizushima, N. (2006). Generation of cell lines with tetracycline-regulated autophagy and a role for autophagy in controlling cell size. *FEBS Lett.* **580**, 2623-2629.

Ichimura, Y., Kirisako, T., Takao, T., Satomi, Y., Shimonishi, Y., Ishihara, N., Mizushima, N., Tanida, I., Kominami, E., Ohsumi, M. et al. (2000). A ubiquitin-like system mediates protein lipidation. *Nature* **408**, 488-492.

Itakura, E. and Mizushima, N. (2010). Characterization of autophagosome formation site by a hierarchical analysis of mammalian Atg proteins. *Autophagy* **6**, 764-776.

Itakura, E. and Mizushima, N. (2011). p62 targeting to the autophagosome formation site requires self-oligomerization but not LC3 binding. *J. Cell Biol.* **192**, 17-27.

Itakura, E., Kishi, C., Inoue, K. and Mizushima, N. (2008). Beclin 1 forms two distinct phosphatidylinositol 3-kinase complexes with mammalian Atg14 and UVRAG. *Mol. Biol. Cell* **19**, 5360-5372.

Johansen, T. and Lamark, T. (2011). Selective autophagy mediated by autophagic adapter proteins. *Autophagy* **7**, 279-296.

Kageyama, S., Omori, H., Saitoh, T., Sone, T., Guan, J. L., Akira, S., Imamoto, F., Noda, T. and Yoshimori, T. (2011). The LC3 recruitment mechanism is separate from Atg9L1-dependent membrane formation in the autophagic response against Salmonella. *Mol. Biol. Cell* **22**, 2290-2300.

Kawajiri, S., Saiki, S., Sato, S., Sato, F., Hatano, T., Eguchi, H. and Hattori, N. (2010). PINK1 is recruited to mitochondria with parkin and associates with LC3 in mitophagy. *FEBS Lett.* **584**, 1073-1079.

Kim, I., Rodriguez-Enriquez, S. and Lemasters, J. J. (2007). Selective degradation of mitochondria by mitophagy. *Arch. Biochem. Biophys.* **462**, 245-253.

Kirkin, V., McEwan, D. G., Novak, I. and Dikic, I. (2009). A role for ubiquitin in selective autophagy. *Mol. Cell* **34**, 259-269.

Kitamura, T., Koshino, Y., Shibata, F., Oki, T., Nakajima, H., Nosaka, T. and Kumagai, H. (2003). Retrovirus-mediated gene transfer and expression cloning: powerful tools in functional genomics. *Exp. Hematol.* **31**, 1007-1014.

Lee, J. Y., Nagano, Y., Taylor, J. P., Lim, K. L. and Yao, T. P. (2010). Disease-causing mutations in parkin impair mitochondrial ubiquitination, aggregation, and HDAC6-dependent mitophagy. *J. Cell Biol.* **189**, 671-679.

Mari, M., Griffith, J., Rieter, E., Krishnappa, L., Klionsky, D. J. and Reggiori, F. (2010). An Atg9-containing compartment that functions in the early steps of autophagosome biogenesis. *J. Cell Biol.* **190**, 1005-1022.

Matsuda, N., Sato, S., Shiba, K., Okatsu, K., Saisho, K., Gautier, C. A., Sou, Y. S., Saiki, S., Kawajiri, S., Sato, F. et al. (2010). PINK1 stabilized by mitochondrial depolarization recruits Parkin to damaged mitochondria and activates latent Parkin for mitophagy. *J. Cell Biol.* **189**, 211-221.

Matsunaga, K., Morita, E., Saitoh, T., Akira, S., Ktistakis, N. T., Izumi, T., Noda, T. and Yoshimori, T. (2010). Autophagy requires endoplasmic reticulum targeting of the PI3-kinase complex via Atg14L. *J. Cell Biol.* **190**, 511-521.

Mizushima, N., Yamamoto, A., Hatano, M., Kobayashi, Y., Kabeya, Y., Suzuki, K., Tokuhisa, T., Ohsumi, Y. and Yoshimori, T. (2001). Dissection of autophagosome formation using Apg5-deficient mouse embryonic stem cells. *J. Cell Biol.* **152**, 657-667.

Mizushima, N., Kuma, A., Kobayashi, Y., Yamamoto, A., Matsubae, M., Takao, T., Natsume, T., Ohsumi, Y. and Yoshimori, T. (2003). Mouse Apg16L, a novel WD-repeat protein, targets to the autophagic isolation membrane with the Apg12-Apg5 conjugate. *J. Cell Sci.* **116**, 1679-1688.

Mizushima, N., Yoshimori, T. and Levine, B. (2010). Methods in mammalian autophagy research. *Cell* **140**, 313-326.

Narendra, D., Tanaka, A., Suen, D. F. and Youle, R. J. (2008). Parkin is recruited selectively to impaired mitochondria and promotes their autophagy. *J. Cell Biol.* **183**, 795-803.

Narendra, D. P., Jin, S. M., Tanaka, A., Suen, D. F., Gautier, C. A., Shen, J., Cookson, M. R. and Youle, R. J. (2010a). PINK1 is selectively stabilized on impaired mitochondria to activate Parkin. *PLoS Biol.* **8**, e1000298.

Narendra, D. P., Kane, L. A., Hauser, D. N., Fearnley, I. M. and Youle, R. J. (2010b). p62/SQSTM1 is required for Parkin-induced mitochondrial clustering but not mitophagy; VDAC1 is dispensable for both. *Autophagy* **6**, 1090-1106.

Noda, T., Kim, J., Huang, W. P., Baba, M., Tokunaga, C., Ohsumi, Y. and Klionsky, D. J. (2000). Apg9p/Cvt7p is an integral membrane protein required for transport vesicle formation in the cvt and autophagy pathways. *J. Cell Biol.* **148**, 465-480.

Okatsu, K., Saisho, K., Shimanuki, M., Nakada, K., Shitara, H., Sou, Y. S., Kimura, M., Sato, S., Hattori, N., Komatsu, M. et al. (2010). p62/SQSTM1 cooperates with Parkin for perinuclear clustering of depolarized mitochondria. *Genes Cells* **15**, 887-900.

Poole, A. C., Thomas, R. E., Yu, S., Vincow, E. S. and Pallanck, L. (2010). The mitochondrial fusion-promoting factor mitofusin is a substrate of the PINK1/parkin pathway. *PLoS ONE* **5**, e10054.

Rakovic, A., Grunewald, A., Seibler, P., Ramirez, A., Kock, N., Orolicki, S., Lohmann, K. and Klein, C. (2010). Effect of endogenous mutant and wild-type PINK1 on Parkin in fibroblasts from Parkinson disease patients. *Hum. Mol. Genet.* **19**, 3124-3137.

Reggiori, F., Tucker, K. A., Stromhaug, P. E. and Klionsky, D. J. (2004). The Atg1-Atg13 complex regulates Atg9 and Atg23 retrieval transport from the pre-autophagosomal structure. *Dev. Cell* **6**, 79-90.

Saitoh, T., Fujita, N., Hayashi, T., Takahara, K., Satoh, T., Lee, H., Matsunaga, K., Kageyama, S., Omori, H., Noda, T. et al. (2009). Atg9a controls dsDNA-driven dynamic translocation of STING and the innate immune response. *Proc. Natl. Acad. Sci. USA* **106**, 20842-20846.

Sou, Y. S., Waguri, S., Iwata, J., Ueno, T., Fujimura, T., Hara, T., Sawada, N., Yamada, A., Mizushima, N., Uchiyama, Y. et al. (2008). The Atg8 conjugation system is indispensable for proper development of autophagic isolation membranes in mice. *Mol. Biol. Cell* **19**, 4762-4775.

Suzuki, K., Kubota, Y., Sekito, T. and Ohsumi, Y. (2007). Hierarchy of Atg proteins in pre-autophagosomal structure organization. *Genes Cells* **12**, 209-218.

Tanaka, A., Cleland, M. M., Xu, S., Narendra, D. P., Suen, D. F., Karbowski, M. and Youle, R. J. (2010). Proteasome and p97 mediate mitophagy and degradation of mitofusins induced by Parkin. *J. Cell Biol.* **191**, 1367-1380.

Tang, H. W., Wang, Y. B., Wang, S. L., Wu, M. H., Lin, S. Y. and Chen, G. C. (2011). Atg1-mediated myosin II activation regulates autophagosome formation during starvation-induced autophagy. *EMBO J.* **30**, 636-651.

Vives-Bauza, C., Zhou, C., Huang, Y., Cui, M., de Vries, R. L., Kim, J., May, J., Tocilescu, M. A., Liu, W., Ko, H. S. et al. (2010). PINK1-dependent recruitment of Parkin to mitochondria in mitophagy. *Proc. Natl. Acad. Sci. USA* **107**, 378-383.

Wang, H., Song, P., Du, L., Tian, W., Yue, W., Liu, M., Li, D., Wang, B., Zhu, Y., Cao, C. et al. (2011). Parkin ubiquitinates Drp1 for proteasome-dependent degradation: implication of dysregulated mitochondrial dynamics in Parkinson's disease. *J. Biol. Chem.* **286**, 11649-11658.

Webber, J. L. and Tooze, S. A. (2010a). Coordinated regulation of autophagy by p38alpha MAPK through mAtg9 and p38IP. *EMBO J.* **29**, 27-40.

Webber, J. L. and Tooze, S. A. (2010b). New insights into the function of Atg9. *FEBS Lett.* **584**, 1319-1326.

Yla-Anttila, P., Vihinen, H., Jokitalo, E. and Eskelinen, E. L. (2009). 3D tomography reveals connections between the phagophore and endoplasmic reticulum. *Autophagy* **5**, 1180-1185.

Yoshii, S. R., Kishi, C., Ishihara, N. and Mizushima, N. (2011). Parkin mediates proteasome-dependent protein degradation and rupture of the outer mitochondrial membrane. *J. Biol. Chem.* **286**, 19630-19640.

Yoshimori, T., Yamagata, F., Yamamoto, A., Mizushima, N., Kabeya, Y., Nara, A., Miwako, I., Ohashi, M., Ohsumi, M. and Ohsumi, Y. (2000). The mouse SKD1, a homologue of yeast Vps4p, is required for normal endosomal trafficking and morphology in mammalian cells. *Mol. Biol. Cell* **11**, 747-763.

Youle, R. J. and Narendra, D. P. (2011). Mechanisms of mitophagy. *Nat. Rev. Mol. Cell Biol.* **12**, 9-14.

Young, A. R. J., Chan, E. Y. W., Hu, X. W., Köchl, R., Crawshaw, S. G., High, S., Hailey, D. W., Lippincott-Schwartz, J. and Tooze, S. A. (2006). Starvation and ULK1-dependent cycling of mammalian Atg9 between the TGN and endosomes. *J. Cell Sci.* **119**, 3888-3900.

Ziviani, E., Tao, R. N. and Whitworth, A. J. (2010). Drosophila parkin requires PINK1 for mitochondrial translocation and ubiquitinates mitofusin. *Proc. Natl. Acad. Sci. USA* **107**, 5018-5023.